International Journal of Rock Mechanics & Mining Sciences 127 (2020) 104213

Contents lists available at ScienceDirect

International Journal of Rock Mechanics and Mining Sciences

journal homepage: http://www.elsevier.com/locate/ijrmms

Incorporating scale effect into a failure criterion for predicting stress-induced overbreak around excavations

A. Delonca [a,b,*], J.A. Vallejos [a]

[a] Department of Mining Engineering, Advanced Mining Technology Center (AMTC), Faculty of Physical and Mathematical Sciences, University of Chile, Chile
[b] Department of Metallurgical and Materials Engineering - Technical University Federico Santa Maria - Santiago - Chile

ARTICLE INFO

Keywords:
Scale effect
Overbreak
Failure criterion

ABSTRACT

The evaluation of the depth of brittle failure around excavations is of major importance in order to optimize the design of underground excavations and ensure the safety of workers and equipment. The current proposed approaches to evaluate it are related to a single scale of study (intact rock or rock mass scale). Therefore, they are scale-dependent, and cannot be applied for all excavation diameter. In this paper, a generalized failure criterion including the scale effect for predicting stress-induced overbreak around excavations is developed. This failure criterion is based on the damage initiation relation ($\sigma_1 = A\sigma_3 + B\sigma_c$). The scale effect is included into it through a relation proposed to evaluate the B parameter and depending on the scale of study. The fit parameters of the relation proposed have been defined considering a database at both rock mass and intact rock scales arising from a literature review. For intact rock scale, the B parameter is defined as a function of the diameter of the excavation, expressed following a potential form. For rock mass scale, the B parameter is defined equal to 0.35, regardless the diameter of the excavation. Based on the proposed B parameter relation, the depth and extension of the brittle failure around excavations can be evaluated for any scale of study.

1. Introduction

The scale effect is a significant characteristic in brittle and quasi-brittle media such as rock.[1] Many authors[2–12] have studied the scale effect with regards to the uniaxial compressive test in different rock types. Moreover, various failure criteria[13–21] have been proposed following investigations of the mechanical behaviour of intact rock. Some of these criteria are extensions of those developed for soils, which do not incorporate the scale effect. One of the most widely used failure criterion is the one proposed by Hoek and Brown.[22] The scale effect has been incorporated into it by assigning a scale effect dependence to the uniaxial compressive strength term, which appears in its definition. However, there was no clear analytical justification for this approach to incorporate the scale effect.[1] Recently, Masoumi et al.[1] proposed to incorporate the scale effect into a multiaxial failure criterion for intact rock by extending the simple two-parameter multiaxial failure criterion proposed by Christensen.[2] This failure criterion allows the scale effect to be included for a more realistic estimation of rock strength with various scales. In this paper, the scale effect is incorporated into a failure criterion for predicting stress-induced overbreak around excavations.

The failure of underground openings in hard rocks depends on the stress state and the fracturing network. Deep mining and tunnelling share the challenge of dealing with intermediate to high both in-situ and induced stresses. These particular stresses conditions, combined to massive blocky rock mass conditions, lead to the initiation of brittle failure surrounding the excavation.[23] The brittle failure can, in particular, lead to stress-induced overbreak. The evaluation of the depth and the extent of the failure is of major importance in order to optimize the design of underground excavations and ensure the safety of workers and equipment[24],.[25]

To estimate the depth of the brittle failure, Martin et al.[26] have used a collection of available tunnel data, compiled by Kaiser et al.[27] They showed that a relationship exists between the depth of failure occurring around an excavation beyond a circumscribed circular profile and the maximum induced tangential stress (σ_{max}) normalized with respect to the laboratory uniaxial compressive strength (σ_c). This empirical approach has since been repeated and confirmed by other studies on tunnel stability in highly stressed ground combined to massive-to-blocky rock mass conditions[24],[28],.[29]

Zoback et al.[30] have studied the depth and the extent of the failure considering a cylindrical hole of 30 cm in a thick, homogeneous, isotropic elastic material. They have evaluated the total minor and

* Corresponding author.
E-mail address: adeline.delonca@usm.cl (A. Delonca).

https://doi.org/10.1016/j.ijrmms.2020.104213
Received 19 August 2016; Received in revised form 21 November 2018; Accepted 9 January 2020
Available online 20 January 2020

major stresses using the Kirsch equations.[31] Then, they have developed equations to evaluate the depth and the extent of the failure, considering the Mohr Coulomb criterion. These equations are controlled by the friction coefficient, the ratio of the distance from the centre of the well to the initial diameter and the extension angle of the failure. This approach has been validated by comparing the results obtained with measured breakout from the well in Auburn, New York. It must be noted that the Mohr Coulomb criterion used in this approach, assumes that the failure occurs on a shear plane experiencing the maximum shear stress. This assumption is typically not valid for brittle, intact rock, in particular when the confining stress is low.[32]

Martin[33] has studied the effect of size and stress gradients on the breakout strength around boreholes, considering previous works[34–38] The physical models proposed revealed that a scale effect is strongly evident at the intact rock scale. When the borehole is at least 75 mm in diameter, the apparent scale effect is absent or significantly reduced. This scale effect increases with decreasing diameter of the borehole. For borehole diameters of less than 15 mm, the tangential stress required to initiate breakouts is greater than $2\sigma_c$.

From the literature review, it is highlighted that the induced-stress failure around excavations has been widely investigated. However, the proposed approaches only focused on tunnels or boreholes cases, and they are scale-dependent. At intact rock scale, a scale effect is highlighted, which is not the case at the rock mass scale. In this paper, a new approach is proposed to incorporate the scale effect into a failure criterion for predicting the stress-induced overbreak around excavations. This failure criterion can be used for any scale of study. The influence of the scale effect is evaluated on both: (1) the depth of failure and (2) the extent of the failure. To do so, the Kirsch equations[31] are used to evaluate the stress state surrounding the excavation. The damage initiation relation is considered as the failure criterion. This relation is approximated by a linear function, related to the total major and minor principal stresses (σ_1 and σ_3), the laboratory uniaxial compressive strength and two parameters, A and B[26,33,39] The B parameter, associated to rock strength, is modified. Then, its influence on the depth and the extent of the failure is evaluated. Moreover, the value of the B parameter corresponding to the empirical database considered by Martin et al.[26] is evaluated. Based on this analysis, a relation of the B parameter is proposed. This relation is based on the published forms proposed to scale the uniaxial compressive strength.

2. Background

The method proposed by Martin et al.[26] to predict the depth of failure is first presented. Then, the damage initiation relation in hard rock and the Kirsch equations are introduced. These two concepts will be combined to evaluate the failure criterion for predicting the brittle failure around excavation and the extension of the failure. Finally, the scale effect in uniaxial compressive strength is presented.

2.1. Depth of stress-induced failure

Martin et al.[26] considered that the failure zone formed around an underground opening is in function of the geometry of the opening, the far-field stresses and the strength of the rock mass. To estimate the depth of failure R_f, they proposed an empirical relation based on the consideration of these parameters. A review of available literature[40–46] identified twenty three cases where the depth of failure and the diameter of each tunnel have been measured (reported in Ref. [26]). These case histories also provided a description of the rock type, the laboratory uniaxial compressive strength σ_c, and the in-situ stress state.

In Fig. 1, the depth of failure (R_f) is normalized to the tunnel diameter a, while the maximum tangential stress (σ_{max}) is normalized to the laboratory uniaxial compressive strength (σ_c). The measured depths of failure given by literature are presented on this Figure.

Fig. 1 implies that the initiation of a stress-induced failure occurs

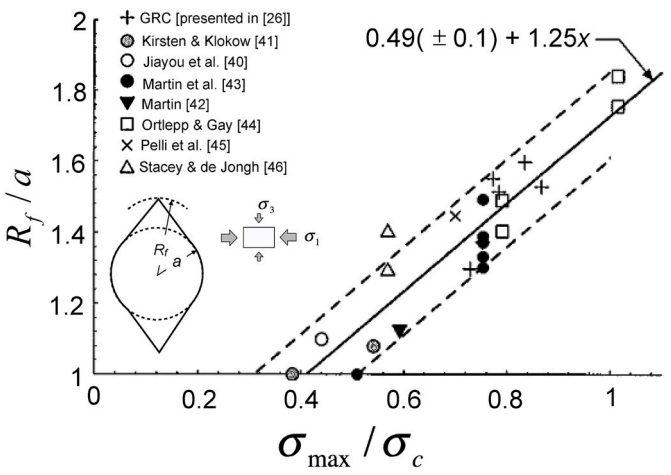

Fig. 1. Predicted depth of failure using measured depths of failure given by Martin et al.[26] Rf is the depth of failure and a is the diameter of the tunnel.

when the ratio σ_{max}/σ_c exceeds 0.4. In other words, the stress-induced failure process begins at stress levels well below the rock's unconfined compressive strength. When this condition occurs, the depth of stress-induced brittle failure around a tunnel in a massive to moderately fractured rock can be approximated by a linear relationship given as (Equation (1)):

$$R_f / a = 0.49(\pm 0.1) + 1.25\ (\sigma_{max} / \sigma_c) \tag{1}$$

2.2. Damage initiation relation in hard rock

Different authors[23,26,33,39,47,48] have demonstrated that the damage initiation relation in hard rock is evaluated by the generic relation:

$$\sigma_1 = A\sigma_3 + B\sigma_c \tag{2}$$

where σ_1 and σ_3 are the total major and minor principal stresses, σ_c is the laboratory uniaxial compressive strength, A is a parameter, varying between 1.0 and 1.6 and is related to friction and B is a parameter, varying between 0.3 and 0.5 for most non-foliated rocks.[47]

The ranges of the A and B parameters of Equation (2) lead to evaluate the upper (peak) and lower (damage) limits of the failure envelopes in hard rock.

2.3. Stresses around a circular excavation

In rock mechanics and rock engineering, the Kirsch equations[31] are widely used to determine the stresses and displacements around a circular excavation in a polar coordinate system. They are applicable for homogeneous, isotropic, continuous and linearly elastic material. The Kirsch equations are expressed as follows[49]:

$$\sigma_r = \frac{P_1 + P_2}{2}\left(1 - \frac{a^2}{r^2}\right) + \frac{P_1 - P_2}{2}\left(1 - \frac{4a^2}{r^2} + \frac{3a^4}{r^4}\right)\cos 2\,\theta \tag{3}$$

$$\sigma_\theta = \frac{P_1 + P_2}{2}\left(1 + \frac{a^2}{r^2}\right) - \frac{P_1 - P_2}{2}\left(1 + \frac{3a^4}{r^4}\right)\cos 2\,\theta \tag{4}$$

$$\tau_{r\theta} = -\frac{P_1 - P_2}{2}\left(1 + \frac{2a^2}{r^2} - \frac{3a^4}{r^4}\right)\sin 2\theta \tag{5}$$

where P_1 and P_2 are the in-situ major and minor stresses, respectively, σ_r, $\sigma_\theta$and $\tau_{r\theta}$ are the radial, tangential and shear stresses around the excavation, a is the diameter of the excavation, r is the distance from the centre of excavation and θ is the azimuth measured from the direction of P_1.

Fig. 2 presents the different parameters used in the Kirsch equations.

The total major and minor principal stresses, σ_1 and σ_3, are evaluated following Equations (6) and (7), respectively.

$$\sigma_1 = \frac{\sigma_r + \sigma_\theta}{2} + \sqrt{\left(\frac{\sigma_r - \sigma_\theta}{2}\right)^2 + \tau_{r\theta}^2} \quad (6)$$

$$\sigma_3 = \frac{\sigma_r + \sigma_\theta}{2} - \sqrt{\left(\frac{\sigma_r - \sigma_\theta}{2}\right)^2 + \tau_{r\theta}^2} \quad (7)$$

2.4. Scale effect in uniaxial compressive strength

The influence of sample size upon rock strength has been widely discussed in literature[4,12,22,50–53]. It is generally assumed that there is a significant reduction in strength with increasing sample size.

Hoek and Brown[12] compiled laboratory test results from samples presenting diameters ranging from 10 mm to 200 mm. They have suggested that the uniaxial compressive strength σ_c of a rock specimen with a diameter of d mm is related to the uniaxial compressive strength σ_{c50} of a 50 mm diameter sample (standard-size specimen) following a potential form (Equation (8)).

$$\sigma_c = \sigma_{c50}\left(\frac{d}{50}\right)^{-k} \quad (8)$$

where k is an exponent variable equal to 0.18.

Different authors[54,55] investigated the effect of scale on the uniaxial compressive strength for samples tests of diameters ranging from 33 mm to 914 mm. The results from these analyses suggested that Equation (8) could also be used to model the observed scale effect. Yoshinaka et al.[4] summarized a research list[10,11,54,56–58] on the scale effect of strength for strong rocks. They highlighted that the exponent k of Equation (8) ranges from about 0.1 to 0.3 for homogeneous hard rock, and from 0.3 to 0.9 for weathered and/or extensively micro-flawed rock.

Martin et al.[59] observed that the Hoek and Brown relation (Equation (8)) significantly under-predicts the strength for normalized diameters (d/50 mm) greater than 3, where the data shows no scale effect (see Fig. 3). They proposed another fit to the normalized data, following an exponential form:

$$\sigma_c = C + \left(\frac{E}{exp\left(\frac{(d/50)}{F}\right)}\right) \quad (9)$$

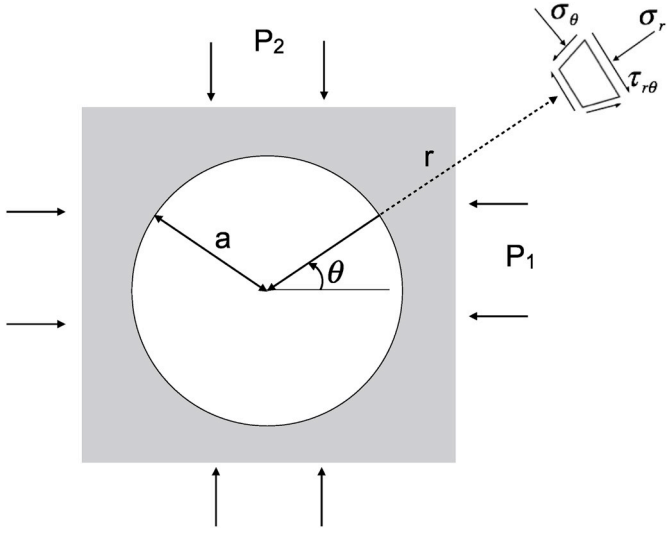

Fig. 2. Stresses around a circular excavation in an isotropic, linearly elastic, homogeneous continuum.

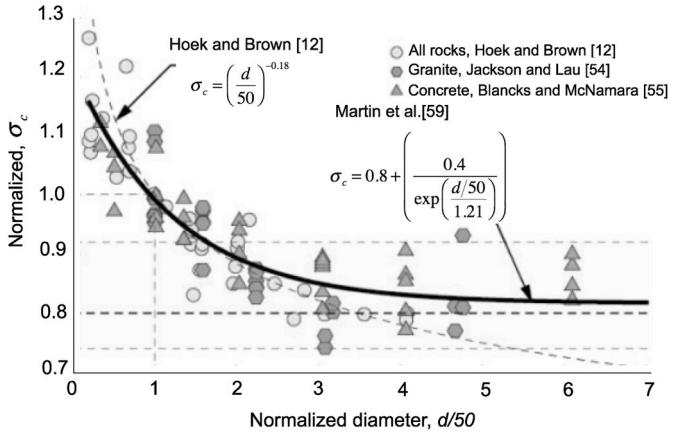

Fig. 3. Influence of specimen size on the strength of intact rock considering the relationships of Hoek and Brown[12] and Martin et al.[59]

where $C = 0.8$, $E = 0.4$ and $F = 1.21$. Equation (9) illustrates that the reduction in σ_c due to the scale effect is limited to 0.8 of the representative laboratory σ_c determined for the intact material.[59] The value 0.8 is also consistent with the original data from Hoek and Brown.[12]

The relations proposed by Hoek and Brown, and by Martin et al. are presented in Fig. 3.

3. Incorporating the scale effect into a failure criterion

The scale effect is incorporated in a failure criterion through the B parameter of the damage initiation relation ($\sigma_1 = A\sigma_3 + B\sigma_c$). In the analysis presented in this paper, the B parameter is modified, and its influence in term of the study scale and rock characteristic is investigated. For each value of the B parameter, the depth and extent of failure is established. Moreover, the best fit of the linear relation proposed by Martin et al.[26] is estimated. This last step leads to evaluate which value of the B parameter is consistent with the historical tunnels database.

To do so, a virtual database is created using the Excel software and its solver tool. Different parameters are defined as fixed components of the database: a, the diameter of the excavation, is taken equal to 1.8 m; ρ, the density of the underground, is taken equal to 2700 kg m^{-3} and σ_c, the laboratory uniaxial compressive strength, is taken equal to 100 Mpa.

Then, two of the database parameters will vary to ensure different in-situ stress conditions of the excavations: K, the ratio of the average horizontal-to-vertical stresses, varies between 1 and 2.1 and z, the depth of the tunnels, varies between 500 and 1500 m.

Based on these parameters, the in-situ major and minor principal stresses are calculated. The horizontal stressσ_h ($\sigma_h = K\sigma_v$) is defined as the major in-situ principal stress. The vertical stressσ_v ($\sigma_v = \rho g z$ where g is the gravity) is defined as the minor in-situ principal stress. Then, the maximum tangential boundary stress σ_{max} ($\sigma_{max} = 3\sigma_h - \sigma_v$) is evaluated. Considering the Kirsch equations, the radial, tangential and shear stresses, σ_r (Equation (3)), σ_θ (Equation (4)) and$\tau_{r\theta}$ (Equation (5), respectively, are calculated. Next, the major and minor principal stresses, σ_1 and σ_3, are evaluated. The rock strengthσ_1^r, defined by the damage initiation relation in hard rock (Equation (2)) is evaluated. Then, σ_1^r is compared to σ_1 through the safety factor σ_1^r/σ_1.

The methodologies followed to evaluate the depth and the extent of failure are presented in the following parts.

3.1. Evaluation of the depth of failure

The angle θ, measured from the horizontal axis, is set to 90°. This angle represents the roof of the excavation. Thus, only the radial σ_r and tangential σ_θ stresses are calculated from Equations (3) and (4). The ratio Rf/a and therefore, the state of stresses σ_1 and σ_3, are modified

using an iterative process on the Excel solver function, until the safety factor σ_1^r/σ_1 is equal to 1. Finally, the graph σ_{max}/σ_c vs. $(R_f/a)_{model}$ is plotted. It's worth noting that $(R_f/a)_{model}$ corresponds to the ratio evaluated based on this procedure. Thus, it can be different from $(R_f/a)_{real}$, calculated using the empirical correlation depending on the historical data.[3]

First, using this procedure, the influence of the *B* parameter on the depth of brittle failure is evaluated. To do so, different values of the *B* parameter of the damage initiation relation (Equation (2)) have been tested, leading to the evaluation of different failure envelopes. The *B* parameter varies between 0.1 and 1, while the *A* parameter is set fixed equal to 1 (lower value of the literature).[33] For each value of the *B* parameter, the relationship between the ratios $(R_f/a)_{model}$ and σ_{max}/σ_c is evaluated.

Then, the best fit with the measured cases considered by Martin et al.[26] is evaluated considering the proposed procedure. To do so, the Residual Sum of Square *RSS* is calculated for different *A* and *B* combinations. The *RSS* is an indicator of performance, taking into account the difference between the $(R_f/a)_{model}$ and $(R_f/a)_{real}$. It is defined as:

$$RSS = \sum_{i=1}^{n}\left((R_f/a)_{model} - (R_f/a)_{real}\right)^2 \quad (10)$$

where *n* is the number of data on the database.

A low *RSS* highlights a good performance of the model. A high *RSS* highlights a bad performance of the model. In the case of the study made, the smaller *RSS* evaluated allowed to define the best fit with the measured brittle failure cases around tunnels.

3.2. Evaluation of the extent of failure

The extent of failure φ_b is equal to 90°- θ, where θ is the angle of failure measured from the horizontal axis. Thus, φ_b can be evaluated by estimating the value of θ (see Fig. 2).

To evaluateφ_b, the angle θ is first set equal to 0. During all the process, the ratio *Rf/a* is considered to be equal to 0. Then, θ is increased using an iterative process of the Excel solver function. Thereby σ_1 and σ_3 (Equation (6) and (7), respectively) are modified. θ is increased until the factor of safety σ_1^r/σ_1 is equal to 1.

The extent of failure is evaluated for different values of the *B* parameter of the damage initiation relation (Equation (2)). To visualize the results, a plot of θ and σ_{max}/σ_c is proposed.

4. Results

4.1. Depth of failure

First, the influence of the *B* parameter of the damage initiation relation is evaluated. The *A* parameter is fixed to 1, and the *B* value is made variable between 0.35 and 1. Fig. 4 shows the predicted depth of failure for different values of *B*. The linear relationship between R_f/a and σ_{max}/σ_c is described by the form y = *m*x+*n*. When the value of *B* increases, the slope *m* of the linear relationship decreases. However, the ordinate value *n* does not change for different values of *B*. The correlation coefficient for each failure envelope is higher than 0.99.

Then, following the methodology presented previously, the best fit with the measured cases compiled by Martin et al.[26] is evaluated. It is obtained for *A* and *B* values equal to 1 and 0.35, respectively. Therefore, the failure envelope corresponding to the historical data is defined by: $\sigma_1 = \sigma_3 + 0.35\sigma_c$. In this case, the *RSS* is equal to 0.27, which is the lower value evaluated, and the coefficient of determination R^2 is equal to 0.98. The linear relationship corresponding to the failure envelope is given by Equation (11) (Fig. 5).

$$R_f/a = 0.54 + 1.15\,(\sigma_{max}/\sigma_c) \quad (11)$$

This result is consistent to the relationship evaluated by Martin et al.[26] (Equation (1)).

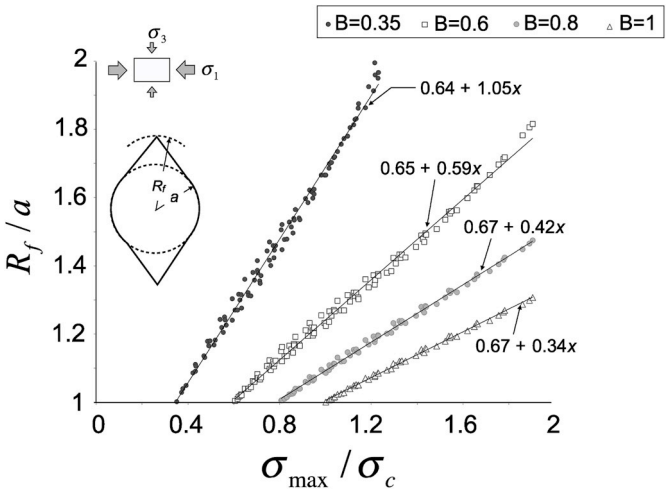

Fig. 4. Comparison between the predicted depth of failure for an A value equal to 1, and different values of B.

4.2. Extent of the failure

The extent of the failure, φ_b, is evaluated in two cases: (1) the *B* parameter is equal to 0.35 and (2) the *B* parameter equal to 0.8.

Fig. 6 shows that for a *B* value equal to 0.35, the extent of the failure ranges globally between 30° and 90°. When considering a *B* value equal to 0.8, the extent of the failure are lower, and ranges globally between 10° and 60°. To be noted that the higher values of σ_{max}/σ_c are related to the higher stress ratio *K*. Finally, for a same value of σ_{max}/σ_c, the extent of the failure gets higher as the stress ratio *K* decreases.

5. The proposed failure criterion

In reference to Fig. 4, the analysis of the *B* parameter highlights a rock mass quality-scale effect. The modification of the *B* parameter corresponds to the modification of the rock characteristics, related to the scale of study. To propose a mathematical function of the *B* parameter consistent with the rock characteristic and the scale of study, previous works are considered. First, the depth of failure around excavations at rock mass scale is investigated. Then, the scale effect at intact rock scale is studied. The proposed failure criterion combined these two

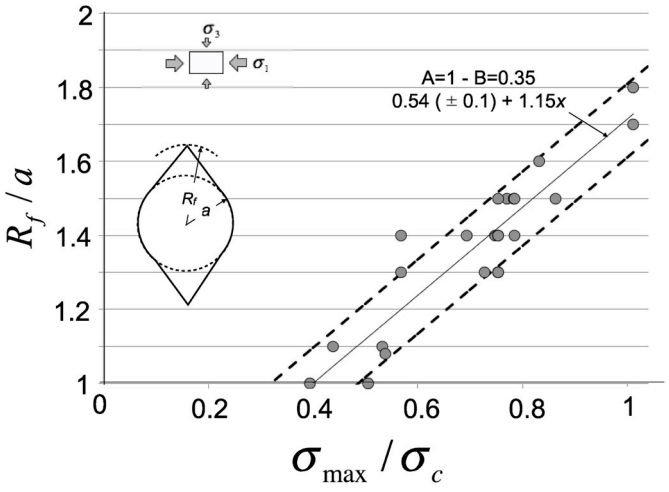

Fig. 5. Failure envelope describing the empirical correlation to predict the depths of failure, considering the measured data collected by Martin et al.[26]

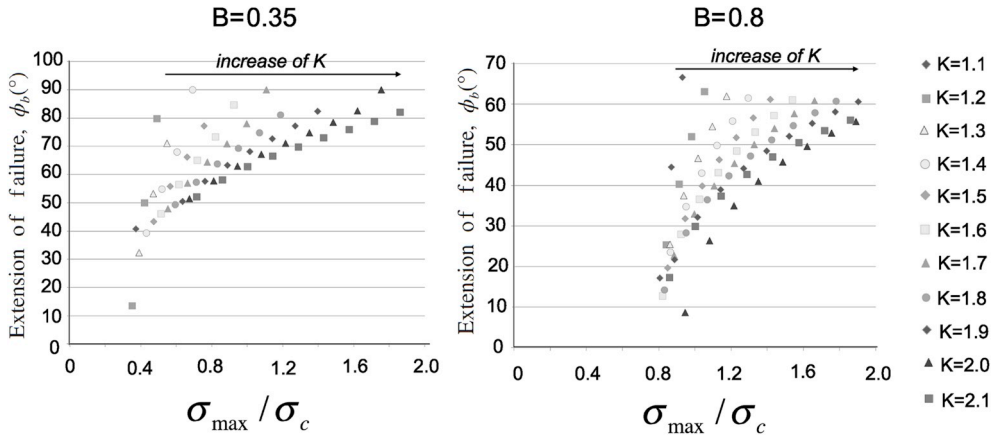

Fig. 6. Extent of failure, φ_b, function of the maximum tangential stress (σ_{max}) normalized to the laboratory uniaxial compressive strength (σ_c). Different values of the stress ratio K are taking into account.

approaches to evaluate a failure criterion consistent for any the scale of study.

5.1. Rock mass scale

Martin et al.[26] studied the depth of failure occurring around excavations in massive-to-blocky rock mass conditions. The diameter of these excavations is of 8 m. Following the methodology presented in this paper, the best fit to the measured historical cases is obtained for a value of the *B* parameter equal to 0.35 (see Fig. 5). Steen et al.[60] analysed two tunnels cases presenting overbreak. The two tunnels have a diameter of 3 and 10 m. These two case studies are presented Fig. 7. In both cases, the value of the *B* parameter associated to them is equal to 0.35. Cai et al.[61] analysed a tunnel with a diameter of 23 m. They defined that $\sigma_1 - \sigma_3 = (0.31 - 0.35)\sigma_c$. These different case studies have diameters ranging from 3 to 23 m. For all these cases, the value of the *B* parameter is close to 0.35.

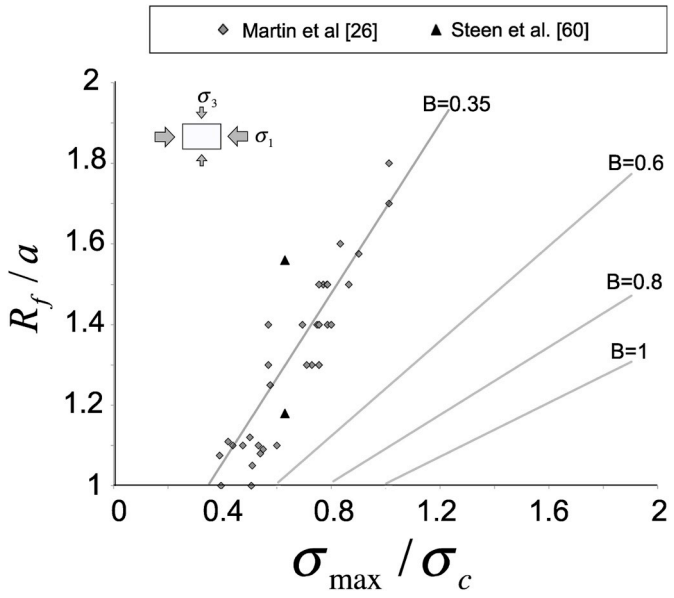

Fig. 7. Data of tunnels[40–46] considered by Martin et al.[26] and by Steen et al.,[60] compared to the predicted depth of failure for a A value equal to 1, and different values of B.

5.2. Intact scale

The effect of size and stress gradients on the breakout strength around boreholes has been examined by many researchers using various physical models[33–38] These models highlighted that the ratio of the calculated tangential stress versus the unconfined compressive strength, σ_{max}/σ_c, at which breakouts initiate depends on the borehole diameter. A scale effect is strongly evident at the intact rock scale for boreholes that are less than 75 mm in diameter (Fig. 8).[33] This scale effect increases with decreasing diameter of the borehole. For borehole diameters of less than 15 mm, the tangential stress required to initiate breakouts is greater than $2\sigma_c$.

5.3. Definition of the proposed failure criterion

The proposed failure criterion, incorporating the scale effect for predicting stress-induced overbreak around excavations, combines the both rock mass and intact rock scales through a relation defining the *B* parameter. As presented previously, a scale effect is strongly evident at the intact rock scale, for boreholes that are less than 75 mm in diameter. To incorporate the scale effect into the *B* parameter relation, both the potential (Equation (8)) and exponential (Equation (9)) models defined to scale the uniaxial compressive strength[12,59] (see §2.4) are considered.

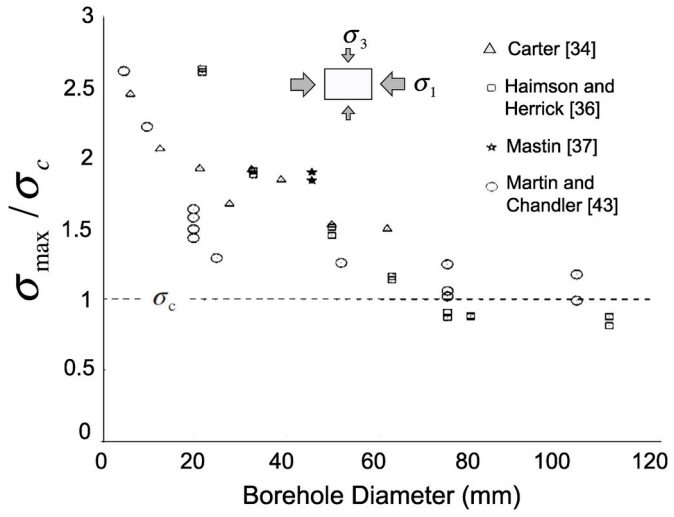

Fig. 8. Ratio of the calculated tangential stress to unconfined compressive strength, $\sigma max/\sigma c$, at which breakouts initiate for various borehole diameters. After Martin33.

These models are used to fit 60 boreholes and tunnels data, compiled from literature[26,33,60,61]. The compiled data present excavation diameters ranging from 5 mm to 23 m.

Fig. 9 presents the best fit to the data considering both the potential and exponential models. Moreover, the originals models proposed by Martin et al.[57] and by Yoshinaka et al.[4] are presented. As a reminder, Yoshinaka et al. described that the exponent k of the potential model ranges from about 0.1 to 0.3 for homogeneous hard rock, and from 0.3 to 0.9 for weathered and/or extensively micro-flawed rock. Note that in Fig. 9, the diameter of the excavation is normalized to 75 mm, which is the limit diameter for which the scale effect is observed[33] (Fig. 8).

Fig. 9 highlights that the original exponential model proposed by Martin et al.[57] and the one proposed by Yoshinaka et al.[4] considering a value of the variable exponent k equal to 0.1 and 0.9 do not fit to the data.

The best fit for the exponential model is evaluated by the following equation:

$$B = C + \left(\frac{E}{exp\left(\frac{(d/75)}{F}\right)} \right) \tag{12}$$

where C is equal to 0.37, E is equal to 2.03 and F is equal to 1.00. Here, d is the diameter of the excavation. The exponential model presents a coefficient of determination R^2 equal to 0.91. Fig. 9 shows that the exponential model is consistent with a parameter B value close to 0.35 for the highest diameter, which can be related to rock mass scale. However, this model assumes that the B parameter is equal to 0.37 for a normalized diameter higher than 4. This hypothesis implies that the rock is intact only until an excavation diameter equal to 300 mm; above this diameter, the rock is at rock mass scale. This hypothesis does not seem to reflect the natural variability of the fracturing around an excavation.

The best fit for the potential model is evaluated by the following equation:

$$B = \alpha \left(\frac{d}{75} \right)^{-k} \tag{13}$$

where α is equal to 1.21 and k is equal to 0.26. The potential model presents a coefficient of determination R^2 equal to 0.94, which is slightly better than when considering the exponential model. The potential model is the best fit to the data, for all excavation diameters. However, the potential model does not represent the constant of the B value (equal to 0.35) at rock mass scale (Fig. 9) properly.

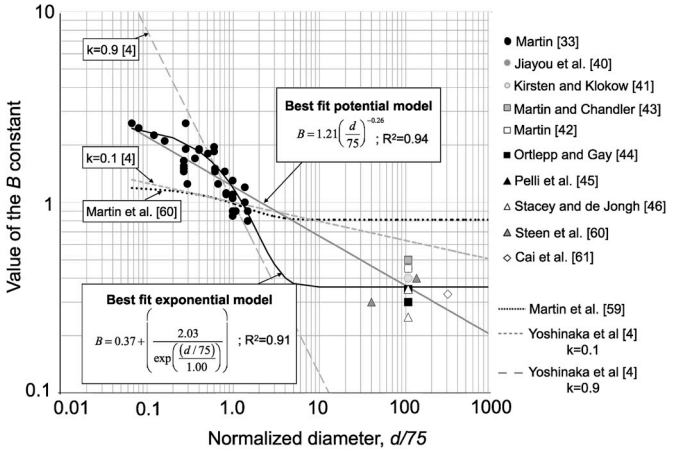

Fig. 9. Values of the B parameter, function of the diameter of the excavation considering boreholes[33–38] and tunnels data[26,60,61]. The horizontal axis represents the logarithm of the normalized diameters of the excavations. The best fit to the data considering potential and exponential models are presented, as well as the originals models[13,57].

Based on the previous observation, the general form of the B parameter is divided into two relations. The first relation is defined at intact rock scale and follows a potential form. The second relation is defined at rock mass scale and presents a B parameter equal to 0.35. To evaluate the limit diameter between the intact rock scale and the rock mass scale, the concept of Representative Elementary Volume (*REV*) is introduced. Cundall et al.[62] have studied the scale effect on rock mass strength, considering the *REV*. They made a review of the work by Schultz,[63] suggesting that the rock mass may be considered as continuum when the problem scale exceeds the block size or fracture spacing by a factor of 10. Therefore, the intact rock scale is maintained until the diameter of the excavation is equal to the diameter of the Representative Elementary Volume (*dREV*), which is equal to 10 times the average block size.

The general relation of the B parameter is described by the following Equation:

$$B = \begin{cases} \alpha \left(\frac{d}{75} \right)^{-k} & d < dREV \\ 0.35\ (\pm\ 0.05) & d \geq dREV \end{cases} \tag{14}$$

where α and k are fitting parameters. The parameter α is equal to 1.18 ($\pm$ 0.2) and the parameter k is equal to 0.29. The fit of the data presents a coefficient of determination R^2 equal to 0.77. d is the diameter of the excavation, in mm, and *dREV* is the limit diameter for which the rock remains at intact scale. It is equal to 10 times the average block size.

5.4. Applicability and limitations

Equation (14) describes the general form proposed to evaluate the B parameter. This equation considers two fitting parameters, α and k, the diameter of the excavation, and the *dREV*, which represents the limit diameter for which the rock mass is considered as continuum. Yoshinaka et al.[4] highlighted that the exponent k of the potential model ranges from 0.1 to 0.3 for homogeneous hard rock, and from 0.3 to 0.9 for weathered and/or extensively micro-flawed rock. The value of the exponent k in Equation (14) is equal to 0.29. Thus, it corresponds to the transition between the two rock types presented previously.

In this work, the Geological Strength Index (GSI) has been considered to evaluate the value of the *dREV*. Cai et al.[23] have related the block volume to the GSI. Thus, it is possible to evaluate an equivalent diameter based on the block volume for a specific value of GSI, and then evaluate the *dREV*, which is equal to 10 times the equivalent diameter. At rock mass scale, the B value is equal to 0.35 ($\pm$ 0.05) (see §5.1). This value corresponds to a GSI of 80.($\pm$5)[61] Considering the graph proposed by Cai et al.[23] (Fig. 10-a), the equivalent diameter evaluated is equal to 500 mm ($\pm$ 200mm). Therefore, the value of the *dREV* is equal to 5000 mm ($\pm$ 2000 mm). Fig. 10-b graphically presents the relation between the B parameter and the normalized diameter. The *dREV* is presented, as well as the corresponding GSI values.

The relation proposed to evaluate the B parameter presents some limitations. This relation is based on the fit of data available in the literature. However, there are no data available for excavations presenting a diameter comprised between 110 mm and 3 m. These data could help to refine the proposed relation, in particular for this range of diameters. Moreover, no data is available for excavations presenting a diameter smaller than 5 mm. Thus, the proposed relation is not valid for diameters smaller than 5 mm. This has to be taken into consideration when evaluating the B parameter.

6. Influence on the extent of the failure

The study of the extent of the failure around excavations has shown that, when considering the rock mass scale, (B parameter equal to 0.35), the extent of the failure ranges between 30° and 89°. When considering

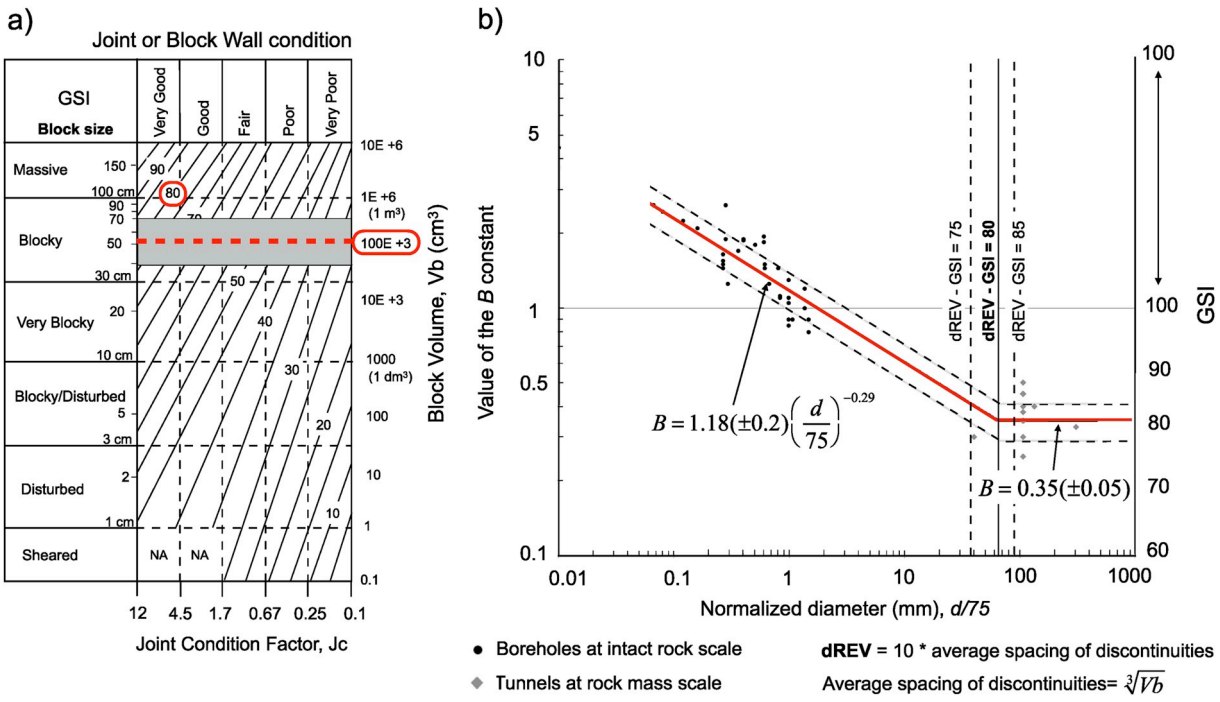

Fig. 10. (a) Relation between the block volume and the Geological Strength Index (GSI) (After Cai et al.[23]). (b) Definition of the relation proposed to evaluate the B parameter.

the intact rock scale (*B* parameter equal to 0.8), the extent of the failure is lower, and ranges between 10° and 60°. Zoback et al.[30] studied the breakout initiation for a borehole considering the Kirsch Equations and the Mohr Coulomb criterion. They present theoretical values of failure extents ranging from 10° to 50°. Moreover, the measured breakout from the well in Auburn, New York present failure extents ranging from 15° to 22°. These results are similar to the one presented in this paper.

7. Concluding remarks

A generalized failure criterion including the scale effect for predicting stress-induced overbreak around excavations has been developed. It is based on the damage initiation relation ($\sigma_1 = A\sigma_3 + B\sigma_c$), and proposes a relation to evaluate the *B* parameter, which depends of the scale of study. The fit parameters of the relation proposed have been defined considering a database at both rock mass and intact rock scales, coming from a literature review. For the intact rock scale, it is defined as a function of the diameter of the excavation, expressed by the potential form proposed to scale the uniaxial compressive strength.[12] For the rock mass scale, the *B* parameter is considered equal to 0.35, regardless the diameter of the excavation. To define the limit diameter between both the intact rock and rock mass scale, the Representative Elementary Volume (*REV*) is introduced. The potential form used to evaluate the *B* parameter is considered until the diameter of the excavation is equal to the diameter of the Representative Elementary Volume (*dREV*), which is equal to 10 times the average block size. The value of the exponent of the potential model is equal to 0.29, which reflects a rock type in transition between an homogeneous hard rock and an extensively micro-flawed rock.[4]

Based on the relation developed, the depth and extent of the brittle failure around excavations can be evaluated for any scale of study. The analysis made on the depth of failure highlighted that, at rock mass scale, the initiation of stress-induced failure occurs when the ratio of the maximum tangential stress normalized to the laboratory uniaxial compressive strength, σ_{max}/σ_c, exceeds 0.4. In other words, the stress-induced failure process begins at stress levels well below the rock's unconfined compressive strength. At intact rock scale, the initiation of stress-induced failure occurs for higher value of the ratio σ_{max}/σ_c than at rock mass scale. For diameters of less than 15 mm, the tangential stress required to initiate breakouts is greater than $2\sigma_c$. Moreover, the analysis indicates that the ratio of the depth of failure versus the radius of the excavation is higher at rock mass scale than at intact rock scale.

The analysis made on the failure's extent shows that the width of the brittle failure is higher at rock mass scale than at intact rock scale. It also highlights that the extent of the failure gets higher as the stress ratio *K* decreases.

It should be noted that the proposed relation is based on the fit of data available in the literature. Nevertheless, no data are available for excavations presenting a diameter between 110 mm and 3 m. These data could help to refine the proposed relation. Moreover, no data is available for excavation presenting a diameter smaller than 5 mm. Thus, the proposed relation is not valid for diameters smaller than 5 mm.

Acknowledgements

The authors would like to acknowledge the financial support of the Advanced Mining Technology Center (AMTC) through the BASAL Project FB-0809.

References

1 Masoumi H, Saydam S, Hagan PC. Incorporating scale effect into a multiaxial failure criterion for intact rock. *Int J Rock Mech Min Sci.* 2016;83:49–56.
2 Christensen RM. Yield functions, damage states, and intrinsic strength. *Math Mech Solids.* 2000;5:285–300.
3 Darlington WJ, Ranjith PG, Choi SK. The effect of specimen size on strength and other properties in laboratory testing of rock and rock-like cementitious brittle materials. *Rock Mech Rock Eng.* 2011;44:513–529.
4 Yoshinaka R, Osada M, Park H, Sasaki T, Sasaki K. Practical determination of mechanical design parameters of intact rock considering scale effect. *Eng Geol.* 2001; 96:173–186.
5 Thuro K, Plinninger RJ, Zäh S, Schütz S. Scale effects in rock strength properties. Part 1: unconfined compressive test and Brazilian test. In: *Rock Mech.- Chall. Soc EUROCK.* 2001:169–174, 2001.
6 Hawkins AB. Aspects of rock strength. *Bull Eng Geol Environ.* 1998;57:17–30.
7 Tsur-Lavie Y, Denekamp SA. Comparison of size effect for different types of strength tests. *Rock Mech.* 1982;15:243–254.

8 Baecher GB, Einstein HH. Size effect in rock testing. *Geophys Res Lett*. 1981;8:671–674.
9 Dey T, Halleck P. Some aspects of size-Effect in rock failure. *Geophys Res Lett*. 1981;8:691–694.
10 Pratt HR, Black AD, Brown WS, Brace WF. The effect of specimen size on the mechanical properties of unjointed diorite. *Int J Rock Mech Min Sci Geomech Abstr*. 1972;9:513–516.
11 Mogi K. The influence of the dimensions of specimens on the fracture strength of rocks: comparison between the strength of rock specimens and that of the Earth's crust. *Bull Earthq Res Inst Univ Tokyo*. 1962;40:175–185.
12 Hoek E, Brown ET. *Underground Excavations in Rock*. London: The Institution of Mining and Metallurgy; 1980.
13 Iwan WD. On a class of models for the yielding behavior of continuous and composite systems. *J Appl Mech*. 1967;34:612–617.
14 Desai CS, Somasundaram S, Frantziskonis G. A hierarchical approach for constitutive modelling of geologic materials. *Int J Numer Anal Methods Geomech*. 1986;10:225–257.
15 Frantziskonis G, Desai CS, Somasundaram S. Constitutive model for non-associative behaviour. *J Eng Mech*. 1986;112:932–946.
16 Liu X, Scarpas A, Blaauwendraad J. Numerical modelling of nonlinear response of soil. Part 2: strain localization investigation on sand. *Int J Solids Struct*. 2005;42:1883–1907.
17 Khan AS, Xiang Y, Huang S. Behavior of Berea sandstone under confining pressure part I: yield and failure surfaces, and nonlinear elastic response. *Int J Plast*. 1991;7:607–624.
18 Kim MK, Lade PV. Single hardening constitutive model for frictional materials. *Comput Geotech*. 1988;5:307–324.
19 Lade PV, Nelson RB. Modelling the elastic behaviour of granular materials. *Int J Numer Anal Methods Geomech*. 1987;11:521–542.
20 Lade PV. Elasto-plastic stress-strain theory for cohesionless soil with curved yield surfaces. *Int J Solids Struct*. 1977;13:1019–1035.
21 Desai CS. A general basis for yield, failure and potential functions in plasticity. *Int J Numer Anal Methods Geomech*. 1980;4:361–375.
22 Hoek E, Brown ET. Practical estimates of rock mass strength. *Int J Rock Mech Min Sci*. 1997;34:165–1186.
23 Cai M, Kaiser PK, Uno H, Tasaka Y, Minami M. Estimation of rock mass deformation modulus and strength of jointed hard rock masses using the GSI system. *Int J Rock Mech Min Sci*. 2004;41:3–19.
24 Diederichs MS, Kaiser PK, Eberhardt E. Damage initiation and propagation in hard rock during tunnelling and the influence of near-face stress rotation. *Int J Rock Mech Min Sci*. 2004;41:785–812.
25 Kaiser PK. Rock mechanics considerations for construction of deep tunnels in brittle rock. In: Rock Mechanics in Underground Construction: ISRM International Symposium 2006: 4th Asian Rock Mechanics Symposium. Singapore; 8-10 November 2006, p. 47-52.
26 Martin CD, Kaiser PK, McCreath DR. Hoek-Brown parameters for predicting the depth of brittle failure around tunnels. *Can Geotech J*. 1999;36:136–151.
27 Kaiser PK. *Canadian Rockburst Support Handbook: Prep. For Sponsors of the Canadian Rockburst Research*. Geomechanics Research Centre; 1996.
28 Kaiser PK, Diederichs MS, Martin CD, Sharp J, Steiner W. Underground works in hard rock tunnelling and mining. In: *ISRM International Symposium*. 2000.
29 Diederichs MS. Mechanistic interpretation and practical application of damage and spalling prediction criteria for deep tunnelling. *Can Geotech J*. 2007;44:1082–1116.
30 Zoback MD, Moos D, Mastin L, Anderson RN. *Well Bore Breakouts and in Situ Stress*. USGS Staff; 1985.
31 Kirsch G. *Die theorie der elastizität und die bedürfnisse der festigkeitslehre*. German: Springer; 1898.
32 Kaiser PK, Amann F, Bewick RP. Overcoming challenges of rock mass characterization for underground construction in deep mines. In: *13th International ISRM Congress*. 2015.
33 Martin CD. The effect of cohesion loss and stress path on brittle rock strength. *Can Geotech J*. 1997;34:698–725.
34 Carter BJ. Size and stress gradient effects on fracture around cavities. *Rock Mech Rock Eng*. 1992;25:167–186.
35 Ewy RT, Cook NGW. Deformation and fracture around cylindrical openings in rock—II. Initiation, growth and interaction of fractures. *Int J Rock Mech Min Sci Geomech Abstr*. 1990;27:409–427.
36 Haimson B, Herrick CG. Borehole breakouts and in situ stress. In: *Proceedings, 12th Annual Energy-Sources Technology Conference and Exhibition, Drilling Symposium*. New York: American Society of Mechanical Engineers; 1989:17–22.
37 Mastin LG. *The Development of Borehole Breakouts in Sandstone*. M.App.Sc. thesis. Berkeley. Calif: Stanford University; 1984.
38 Hoek E. *Rock Fracture under Static Stress Conditions*. CSIR, Technical Report; 1965.
39 Brace WF, Martin RJ. A test of the law of effective stress for crystalline rocks of low porosity. *Int J Rock Mech Min Sci Geomech Abstr*. 1968;5:415–426.
40 Jiayou L, Lihui D, Chengjie Z, Zebin W. The brittle failure of rock around underground openings. In: *ISRM International Symposium*. 1989.
41 Kirsten HAD, Klokow JW. Control of fracturing in mine rock passes. In: *4th ISRM Congress*. 1979.
42 Martin CD. Failure observations and in situ stress domains at the Underground Research Laboratory. In: *ISRM International Symposium*. 1989.
43 Martin CD, Chandler NA. The progressive fracture of Lac du Bonnet granite. *Int J Rock Mech Min Sci Geomech Abstr*. 1994;31:643–659.
44 Ortlepp WD, Gay NC. Performance of an experimental tunnel subjected to stresses ranging from 50 MPa to 230 MPa. In: *Proceedings of the ISRM Symposium: Design and Performance of Underground Excavations*. 1984:337–346.
45 Pelli F, Kaiser PK, Morgenstern NR. An interpretation of ground movements recorded during construction of the Donkin-Morien tunnel. *Can Geotech J*. 1991;28:239–254.
46 Stacey T, De Jongh CL. Stress fracturing around a deep-level bored tunnel. *J. South Afr. Inst. Min. Metall. Dec*. 1977;2:124–133.
47 Diederichs MS, Carvalho JL, Carter TG. A modified approach for prediction of strength and post yield behaviour for high GSI rock masses in strong, brittle ground. In: *Proceedings of the 1st Canada-US Rock Mechanics Symposium*. Vancouver: Canada; 2007.
48 Holcomb DJ, Martin RJI. *Determining Peak Stress History Using Acoustic Emissions. Sandia National Labs*. Albuquerque, NM (United States): Applied Research Associates, Inc.; 1985. South Royalton, VT (United States).
49 Goodman RE. *Introduction to Rock Mechanics*. New York: Wiley; 1989.
50 Evans I, Pomeroy CD. The strength of cubes of coal in uniaxial compression. *Mech Prop Non-Metallic Brittle Mater*. 1958;2:5–28.
51 Jaeger JC, Cook NG, Zimmerman R. *Fundamentals of Rock Mechanics*. John Wiley & Sons; 2009.
52 Bazant ZP. Scaling laws in mechanics of failure. *J Eng Mech*. 1993;119:1828–1844.
53 Tsoutrelis CE, Exadaktylos GF. Effect of rock discontinuities on certain rock strength and fracture energy parameters under uniaxial compression. *Geotech Geol Eng*. 1993;11:81–105.
54 Jackson R, Lau JSO. The effect of specimen size on the mechanical properties of Lac du Bonnet grey granite. In: *Proc. 1st. Int. Workshop on Scale Effects in Rock Masses*. Norway: Loen; 1990:165–174.
55 Blanks RF, McNamara CC. Mass concrete tests in large cylinders. *ACI J Proc*. 1935:280–303.
56 Lundborg N. The strength-size relation of granite. *Int J Rock Mech Min Sci Geomech Abstr*. 1967;4:269–272.
57 Nishimatsu Y, Yamaguchi U, Motosugi K, Morita M. The size effect and experimental error of the strength of rocks. *J. Soc. Mater. Sci. Jpn*. 1969;18:1019–1025.
58 Herget G, Unrug K. In situ rock strength from triaxial testing. *Int J Rock Mech Min Sci Geomech Abstr*. 1976;13:299–302.
59 Martin CD, Lu Y, Lan H. Scale effects in a synthetic rock mass. *Harmonising Rock Mech Rock Eng*. 2012;1:473–478.
60 de Steen BV, Vervoort A, Napier JAL, Durrheim RJ. Implementation of a flaw model to the fracturing around a vertical shaft. *Rock Mech Rock Eng*. 2003;36:143–161.
61 Cai M, Kaiser PK, Tasaka Y, Maejima T, Morioka H, Minami M. Generalized crack initiation and crack damage stress thresholds of brittle rock masses near underground excavations. *Int J Rock Mech Min Sci*. 2004;4:833–847.
62 Cundall PA, Pierce M, Ivars DM. Quantifying the size effect of rock mass strength. In: *Proceedings of the 1st Southern Hemisphere International Rock Mechanics Symposium*. Australia: Perth; 2008.
63 Schultz RA. Relative scale and the strength and deformability of rock masses. *J Struct Geol*. 1996;18:1139–1149.